

# Observation of the $D_1(2420) \rightarrow D\pi^+\pi^-$ decays.

K. Abe,<sup>7</sup> K. Abe,<sup>40</sup> I. Adachi,<sup>7</sup> H. Aihara,<sup>42</sup> M. Akatsu,<sup>20</sup> D. Anipko,<sup>1</sup> Y. Asano,<sup>45</sup> T. Aushev,<sup>11</sup> T. Aziz,<sup>38</sup> S. Bahinipati,<sup>4</sup> A. M. Bakich,<sup>37</sup> S. Banerjee,<sup>38</sup> I. Bedny,<sup>1</sup> U. Bitenc,<sup>12</sup> I. Bizjak,<sup>12</sup> S. Blyth,<sup>24</sup> A. Bondar,<sup>1</sup> A. Bozek,<sup>25</sup> M. Bračko,<sup>7,18,12</sup> J. Brodzicka,<sup>25</sup> P. Chang,<sup>24</sup> Y. Chao,<sup>24</sup> A. Chen,<sup>22</sup> K.-F. Chen,<sup>24</sup> W. T. Chen,<sup>22</sup> B. G. Cheon,<sup>3</sup> R. Chistov,<sup>11</sup> S.-K. Choi,<sup>5</sup> Y. Choi,<sup>36</sup> A. Chuvikov,<sup>32</sup> J. Dalseno,<sup>19</sup> M. Danilov,<sup>11</sup> M. Dash,<sup>46</sup> A. Drutskoy,<sup>4</sup> S. Eidelman,<sup>1</sup> V. Eiges,<sup>11</sup> F. Fang,<sup>6</sup> S. Fratina,<sup>12</sup> N. Gabyshev,<sup>1</sup> A. Garmash,<sup>32</sup> T. Gershon,<sup>7</sup> G. Gokhroo,<sup>38</sup> B. Golob,<sup>17,12</sup> J. Haba,<sup>7</sup> N. C. Hastings,<sup>7</sup> K. Hayasaka,<sup>20</sup> H. Hayashii,<sup>21</sup> M. Hazumi,<sup>7</sup> T. Higuchi,<sup>7</sup> L. Hinz,<sup>16</sup> T. Hokuue,<sup>20</sup> Y. Hoshi,<sup>40</sup> S. Hou,<sup>22</sup> W.-S. Hou,<sup>24</sup> T. Iijima,<sup>20</sup> A. Imoto,<sup>21</sup> K. Inami,<sup>20</sup> A. Ishikawa,<sup>7</sup> R. Itoh,<sup>7</sup> Y. Iwasaki,<sup>7</sup> J. H. Kang,<sup>47</sup> J. S. Kang,<sup>14</sup> P. Kapusta,<sup>25</sup> S. U. Kataoka,<sup>21</sup> N. Katayama,<sup>7</sup> H. Kawai,<sup>2</sup> T. Kawasaki,<sup>27</sup> H. Kichimi,<sup>7</sup> H. J. Kim,<sup>15</sup> J. H. Kim,<sup>36</sup> S. K. Kim,<sup>35</sup> S. M. Kim,<sup>36</sup> K. Kinoshita,<sup>4</sup> P. Koppenburg,<sup>7</sup> S. Korpar,<sup>18,12</sup> P. Križan,<sup>17,12</sup> P. Krokovny,<sup>1</sup> C. C. Kuo,<sup>22</sup> A. Kuzmin,<sup>1</sup> Y.-J. Kwon,<sup>47</sup> G. Leder,<sup>10</sup> S. H. Lee,<sup>35</sup> T. Lesiak,<sup>25</sup> J. Li,<sup>34</sup> S.-W. Lin,<sup>24</sup> D. Liventsev,<sup>11</sup> J. MacNaughton,<sup>10</sup> G. Majumder,<sup>38</sup> F. Mandl,<sup>10</sup> T. Matsumoto,<sup>43</sup> A. Matyja,<sup>25</sup> W. Mitaroff,<sup>10</sup> H. Miyata,<sup>27</sup> R. Mizuk,<sup>11</sup> T. Nagamine,<sup>41</sup> Y. Nagasaka,<sup>8</sup> E. Nakano,<sup>28</sup> Z. Natkaniec,<sup>25</sup> S. Nishida,<sup>7</sup> O. Nitoh,<sup>44</sup> S. Ogawa,<sup>39</sup> T. Ohshima,<sup>20</sup> T. Okabe,<sup>20</sup> S. Okuno,<sup>13</sup> S. L. Olsen,<sup>6</sup> W. Ostrowicz,<sup>25</sup> H. Ozaki,<sup>7</sup> P. Pakhlov,<sup>11</sup> H. Palka,<sup>25</sup> C. W. Park,<sup>36</sup> N. Parslow,<sup>37</sup> R. Pestotnik,<sup>12</sup> L. E. Pilonen,<sup>46</sup> A. Poluektov,<sup>1</sup> H. Sagawa,<sup>7</sup> Y. Sakai,<sup>7</sup> N. Sato,<sup>20</sup> T. Schietinger,<sup>16</sup> O. Schneider,<sup>16</sup> J. Schumann,<sup>24</sup> S. Semenov,<sup>11</sup> K. Senyo,<sup>20</sup> R. Seuster,<sup>6</sup> H. Shibuya,<sup>39</sup> B. Shwartz,<sup>1</sup> J. B. Singh,<sup>30</sup> A. Somov,<sup>4</sup> N. Soni,<sup>30</sup> R. Stamen,<sup>7</sup> S. Stanič,<sup>45,\*</sup> M. Starič,<sup>12</sup> K. Sumisawa,<sup>29</sup> T. Sumiyoshi,<sup>43</sup> S. Suzuki,<sup>33</sup> S. Y. Suzuki,<sup>7</sup> O. Tajima,<sup>7</sup> F. Takasaki,<sup>7</sup> K. Tamai,<sup>7</sup> N. Tamura,<sup>27</sup> M. Tanaka,<sup>7</sup> Y. Teramoto,<sup>28</sup> X. C. Tian,<sup>31</sup> T. Tsukamoto,<sup>7</sup> S. Uehara,<sup>7</sup> T. Uglov,<sup>11</sup> K. Ueno,<sup>24</sup> S. Uno,<sup>7</sup> K. E. Varvell,<sup>37</sup> S. Villa,<sup>16</sup> C. C. Wang,<sup>24</sup> C. H. Wang,<sup>23</sup> M. Watanabe,<sup>27</sup> B. D. Yabsley,<sup>46</sup> A. Yamaguchi,<sup>41</sup> Y. Yamashita,<sup>26</sup> M. Yamauchi,<sup>7</sup> J. Ying,<sup>31</sup> Y. Yusa,<sup>41</sup> C. C. Zhang,<sup>9</sup> J. Zhang,<sup>7</sup> L. M. Zhang,<sup>34</sup> Z. P. Zhang,<sup>34</sup> V. Zhilich,<sup>1</sup> and D. Žontar<sup>17,12</sup>

(The Belle Collaboration)

<sup>1</sup>*Budker Institute of Nuclear Physics, Novosibirsk*

<sup>2</sup>*Chiba University, Chiba*

<sup>3</sup>*Chonnam National University, Kwangju*

<sup>4</sup>*University of Cincinnati, Cincinnati, Ohio 45221*

<sup>5</sup>*Gyeongsang National University, Chinju*

<sup>6</sup>*University of Hawaii, Honolulu, Hawaii 96822*

<sup>7</sup>*High Energy Accelerator Research Organization (KEK), Tsukuba*

<sup>8</sup>*Hiroshima Institute of Technology, Hiroshima*

<sup>9</sup>*Institute of High Energy Physics, Chinese Academy of Sciences, Beijing*

<sup>10</sup>*Institute of High Energy Physics, Vienna*

<sup>11</sup>*Institute for Theoretical and Experimental Physics, Moscow*

<sup>12</sup>*J. Stefan Institute, Ljubljana*

<sup>13</sup>*Kanagawa University, Yokohama*

<sup>14</sup>*Korea University, Seoul*

<sup>15</sup>*Kyungpook National University, Taegu*

<sup>16</sup>*Swiss Federal Institute of Technology of Lausanne, EPFL, Lausanne*

<sup>17</sup>*University of Ljubljana, Ljubljana*

<sup>18</sup>*University of Maribor, Maribor*

<sup>19</sup>*University of Melbourne, Victoria*

<sup>20</sup>*Nagoya University, Nagoya*

<sup>21</sup>*Nara Women's University, Nara*

<sup>22</sup>*National Central University, Chung-li*

<sup>23</sup>*National United University, Miao Li*

<sup>24</sup>*Department of Physics, National Taiwan University, Taipei*

<sup>25</sup>*H. Niewodniczanski Institute of Nuclear Physics, Krakow*

<sup>26</sup>*Nihon Dental College, Niigata*

<sup>27</sup>*Niigata University, Niigata*

<sup>28</sup>*Osaka City University, Osaka*

<sup>29</sup>*Osaka University, Osaka*

<sup>30</sup>*Panjab University, Chandigarh*

<sup>31</sup>*Peking University, Beijing*

<sup>32</sup>*Princeton University, Princeton, New Jersey 08545*

<sup>33</sup>*Saga University, Saga*

<sup>34</sup>*University of Science and Technology of China, Hefei*

<sup>35</sup>Seoul National University, Seoul

<sup>36</sup>Sungkyunkwan University, Suwon

<sup>37</sup>University of Sydney, Sydney NSW

<sup>38</sup>Tata Institute of Fundamental Research, Bombay

<sup>39</sup>Toho University, Funabashi

<sup>40</sup>Tohoku Gakuin University, Tagajo

<sup>41</sup>Tohoku University, Sendai

<sup>42</sup>Department of Physics, University of Tokyo, Tokyo

<sup>43</sup>Tokyo Metropolitan University, Tokyo

<sup>44</sup>Tokyo University of Agriculture and Technology, Tokyo

<sup>45</sup>University of Tsukuba, Tsukuba

<sup>46</sup>Virginia Polytechnic Institute and State University, Blacksburg, Virginia 24061

<sup>47</sup>Yonsei University, Seoul

We report on the first observation of  $D_1(2420) \rightarrow D\pi^+\pi^-$  decays (where the contribution from the dominant known  $D_1 \rightarrow D^*\pi$  decay mode is excluded) in the  $B \rightarrow D_1\pi$  decays. The observation is based on  $15.2 \times 10^7 B\bar{B}$  events collected with the Belle detector at the KEKB collider. We also set 90% confidence level upper limits for the  $D_2^* \rightarrow D^{(*)}\pi^+\pi^-$  and  $D_1 \rightarrow D^*\pi^+\pi^-$  decays in the  $B \rightarrow D_2^*(2460)\pi$  and  $B \rightarrow D_1(2420)\pi$  decays, respectively.

PACS numbers: 13.25.Hw, 14.40.Lb

The  $D_1 \rightarrow D^*\pi$  decay is currently known to be the primary decay mode of the  $D_1(2420)$  meson [1]. However, the transitions  $D_1 \rightarrow D\pi\pi$  via other intermediate quasi-two-body resonance states or via non-resonant decays are possible and may contribute to the  $D_1$  total width. Measurements of their branching ratios and analysis of the decay dynamics are particularly relevant to a study of production rates of various  $D^{**}$  excitations in  $B$  decays.

The ratio of the branching fractions  $R = \mathcal{B}(B^- \rightarrow D_2^{*0}\pi^-)/\mathcal{B}(B^- \rightarrow D_1^0\pi^-)$  is calculated in HQET and the factorization approximation in Refs. [2, 3]. In Ref. [2],  $R$  is found to depend on the values of the subleading Isgur-Wise functions ( $\hat{\tau}_{1,2}$ ) describing  $\Lambda_{QCD}/m_c$  corrections; thus measurement of  $R$  can be used to estimate the subleading functions. In Ref. [3], some of the subleading terms are estimated and the ratio is determined to be  $R \approx 0.35 \left| (1 + \delta_8^{D^2}) / (1 + \delta_8^{D^1}) \right|$ , where  $\delta_8^{D^1(D^2)}$  are non-factorizable corrections that are expected to be small.

The first observation of  $D^{**}$  (denotes  $P$ -wave  $D$  excitations) production in  $B$  decays was reported by CLEO [4]. From their studies and the measurement of the ratio  $\mathcal{B}(D_2^{*0} \rightarrow D^+\pi^-)/\mathcal{B}(D_2^{*0} \rightarrow D^{*+}\pi^-)$  [5, 6] the  $R$  value was determined to be  $R = 1.8 \pm 0.8$ , where it was assumed that decays of  $D_1$  and  $D_2^*$  mesons are saturated by the two-body  $D\pi$ ,  $D^*\pi$  modes. Recently the branching fractions for the decays  $B \rightarrow D^{**}\pi \rightarrow D^{(*)}\pi\pi$  have been measured with better accuracy [7], resulting in  $R = 0.77 \pm 0.15$ . The existence of  $D_{(1,2)}$  decay channels other than  $D_1 \rightarrow D^{(*)}\pi$  can also affect the  $R$  value, either decreasing or increasing the currently observed  $2.8\sigma$  difference between the prediction and experimental results.

In this Letter we report the first observation of the  $D_1^+ \rightarrow D^+\pi^-\pi^+$  and  $D_1^0 \rightarrow D^0\pi^-\pi^+$  decays. The  $D_1$  mesons were reconstructed from the  $\bar{B}^0 \rightarrow D_1^+\pi^-$  and  $B^- \rightarrow D_1^0\pi^-$  decays, respectively. The results are based

on a sample of  $15.2 \times 10^7 B\bar{B}$  pairs produced at the KEKB asymmetric energy  $e^+e^-$  collider [8]. The inclusion of charge conjugate states is implicit throughout this report.

The Belle detector has been described elsewhere [9]. Charged tracks are selected with a set of requirements based on the average number of hits in the central drift chamber (CDC) and on the distance of the closest approach to the interaction point. Track momentum transverse to the beam axis of at least 0.05 GeV/ $c$  is required for all tracks in order to reduce the combinatorial background. For charged particle identification (PID), the combined information from specific ionization in the CDC ( $dE/dx$ ), time-of-flight scintillation counters and aerogel Čerenkov counters is used. Charged kaons are selected with PID criteria that have an efficiency of 88%, a pion misidentification probability of 8%, and negligible contamination from protons. All charged tracks with PID responses consistent with a pion hypothesis that are not positively identified as electrons are considered as pion candidates. Photon candidates are selected from calorimeter showers not associated with charged tracks. An energy deposition of at least 30 MeV and a photon-like shape are required for each candidate. Pairs of photons with an invariant mass within 12 MeV/ $c^2$  ( $\sim 2.5\sigma$ ) of the  $\pi^0$  nominal mass [1] are considered as  $\pi^0$  candidates.

We reconstruct  $D^0(D^+)$  mesons in the  $K^-\pi^+$  ( $K^-\pi^+\pi^+$ ) decay channel and require the invariant mass to be within 15 MeV/ $c^2$  ( $\sim 3\sigma$ ) of the  $D^0(D^+)$  mass. Then,  $D^{*0}(D^{*+})$  mesons are reconstructed in the  $D^0\pi^0(D^0\pi^+)$  decay mode. The calculated mass difference between  $D^{*0}(D^{*+})$  and  $D^0$  candidates is required to be within 2 (1.5) MeV/ $c^2$  ( $\sim 2.5\sigma$ ) of the expected value [1]. For  $D^* \rightarrow D^0\pi$  decays the  $D^0 \rightarrow K^-\pi^+\pi^+\pi^-$  mode is also included (the same  $D^*$  parameters were used as above).

TABLE I: Number of events, efficiencies and branching fraction products of  $B \rightarrow D^{**}\pi, D^{**} \rightarrow D^{(*)}\pi^+\pi^-$  decays.

Mode	$N_{sig}$	$\varepsilon$ ( $10^{-2}$ )	$\mathcal{B}$ ( $10^{-4}$ )	Significance
$B^- \rightarrow D_1^0\pi^-, D_1^0 \rightarrow D^0\pi^-\pi^+$	$151 \pm 24$	14.1	$(1.85 \pm 0.29 \pm 0.35_{-0.46}^{+0.0})$	$8.7\sigma$
$\bar{B}^0 \rightarrow D_1^+\pi^-, D_1^+ \rightarrow D^+\pi^-\pi^+$	$124 \pm 20$	9.9	$(0.89 \pm 0.15 \pm 0.17_{-0.26}^{+0.0})$	$10\sigma$
$B^- \rightarrow D_1^0\pi^-, D_1^0 \rightarrow D^{*0}\pi^+\pi^-$	$< 1.2$	2.2	$< 0.06$	-
$\bar{B}^0 \rightarrow D_1^+\pi^-, D_1^+ \rightarrow D^{*+}\pi^+\pi^-$	$< 12.0$	3.4	$< 0.33$	-
$B^- \rightarrow D_2^{*0}\pi^-, D_2^{*0} \rightarrow D^{*0}\pi^+\pi^-$	$< 4.4$	2.2	$< 0.22$	-
$\bar{B}^0 \rightarrow D_2^{*+}\pi^-, D_2^{*+} \rightarrow D^{*+}\pi^+\pi^-$	$< 9.0$	3.4	$< 0.24$	-

We combine  $D^{(*)}$  candidates with  $\pi^-\pi^-\pi^+$  to form  $B$  mesons. Candidate events are identified by their center-of-mass (CM) energy difference,  $\Delta E = (\sum_i E_i) - E_{beam}$ , and the beam constrained mass,  $M_{bc} = \sqrt{E_{beam}^2 - (\sum_i \vec{p}_i)^2}$ , where  $E_{beam}$  is the beam energy and  $\vec{p}_i$  and  $E_i$  are the momenta and energies of the decay products of the  $B$  meson in the CM frame. We define the signal region as  $5.273 \text{ GeV}/c^2 < M_{bc} < 5.285 \text{ GeV}/c^2$  and  $|\Delta E| < 25 \text{ MeV}$ . The sidebands are defined as  $5.273 \text{ GeV}/c^2 < M_{bc} < 5.285 \text{ GeV}/c^2$  and  $25 \text{ MeV} < |\Delta E| < 50 \text{ MeV}$ . If there is more than one  $B$  candidate in an event, the one with  $D^{(*)}$  mass closest to the nominal value and the best  $\pi^-\pi^-\pi^+$  vertex is chosen. We use Monte Carlo (MC) simulation to model the detector response and determine the acceptance [10].

Variables that characterize the event topology calculated in the CM frame are used to suppress background from the two-jet-like  $e^+e^- \rightarrow q\bar{q}$  continuum process. We require  $|\cos\theta_{thr}| < 0.80$ , where  $\theta_{thr}$  is the angle between the thrust axis of the  $B$  candidate and that of the rest of the event; this eliminates 77% of the continuum background while retaining 78% of the signal events. We also define a Fisher discriminant,  $\mathcal{F}$ , which is based on the production angle of the  $B$  candidate, the angle of the thrust axis with respect to the beam axis, and nine parameters that characterize the momentum flow in the event [11]. We impose a requirement on  $\mathcal{F}$  that rejects 67% of the remaining continuum background and retains 83% of the signal.

To suppress the large contribution from the dominant  $D_1 \rightarrow D^*\pi \rightarrow D\pi\pi$  decay mode we apply a requirement on the invariant mass of the relevant  $D\pi$  combination  $|(m_{D\pi} - m_D) - (m_{D^*}^{PDG} - m_D^{PDG})| > 6 \text{ MeV}/c^2$  [1] ( $10\sigma$ ).

The  $\Delta E$  and  $M_{D^{(*)}\pi\pi}$  distributions for the selected  $B \rightarrow D_1\pi, D_1 \rightarrow D^{(*)}\pi\pi$  candidates are shown in Fig. 1. To plot the  $\Delta E$  distributions, we require  $M_{bc}$  to lie in the signal region with an additional requirement  $|M_{D^{(*)}\pi\pi} - M_{D_1}| < 25 \text{ MeV}/c^2$ , where  $M_{D_1}$  is the  $D_1$  world average mass value; for the  $M_{D^{(*)}\pi\pi}$  distributions we select events from the  $\Delta E$  signal region. (Although there are two  $D\pi^+\pi^-$  combinations, they are kinematically separated in the  $D_1$  mass region.) Clear signals are observed for  $B^- \rightarrow D_1^0\pi^-, D_1^0 \rightarrow D^0\pi^-\pi^+$  and  $\bar{B}^0 \rightarrow D_1^+\pi^-, D_1^+ \rightarrow D^+\pi^-\pi^+$  decays. For branch-

ing fraction calculations we use signal yields determined from the fit to  $M_{D\pi\pi}$  distributions as it allows us to directly estimate a possible contribution from  $B \rightarrow D_2\pi, D_2 \rightarrow D\pi\pi$  decay. The signal shape distribution is parameterized by a convolution of a resolution Gaussian ( $\sigma = 2.5 \text{ MeV}/c^2$ ) with a signal Breit-Wigner function; the background is represented by a linear function. The  $D_1$  mass and width determined from the fit are  $M_{D_1^0} = 2426 \pm 3 \pm 1 \text{ MeV}/c^2$  (statistical and systematic error, respectively),  $\Gamma_{D_1^0} = 24 \pm 7 \pm 8 \text{ MeV}/c^2$  for  $D_1^0$  and  $M_{D_1^+} = 2421 \pm 2 \pm 1 \text{ MeV}/c^2$ ,  $\Gamma_{D_1^+} = 21 \pm 5 \pm 8 \text{ MeV}/c^2$  for  $D_1^+$ ; these are consistent with the world average values [1]. The signal yields are given in Table I (in the cited branching ratios the first and second errors are statistical and systematic; where a third error given is due to model uncertainty). For the  $B \rightarrow D_1\pi \rightarrow D^*\pi^-\pi^-\pi^+$  decay channels, we do not observe statistically significant signals and thus determine 90% CL upper limits [12] for their branching fractions. In the fit to the  $M_{D^*\pi\pi}$  distribution, we fix the  $D_1$  mass and width at their world average values. The statistical significance of signals quoted in Table I is defined as  $\sqrt{-2 \ln(L_0/L_{max})}$ , where  $L_{max}$  and  $L_0$  denote the maximum likelihood with the nominal signal yield and with the signal yield fixed at zero, respectively.

To account for contamination from other possible  $D_1$  production mechanisms (such as  $e^+e^- \rightarrow c\bar{c}$  continuum production or semileptonic  $B \rightarrow D_1 l \bar{\nu}$  decays), we fit the  $M_{D\pi\pi}$  distribution for events in the  $\Delta E$  sidebands. In this fit, we fix the  $D_1$  mass and width at their world average values. The fits give  $-6 \pm 8$  events for the  $D_1^0$  and  $10 \pm 11$  events for the  $D_1^+$ .

The  $B \rightarrow D_2^*(2460)\pi, D_2^* \rightarrow D\pi^+\pi^-$  decay may also contribute to the  $B \rightarrow D\pi^-\pi^-\pi^+$  final state. To analyse a possible effect, we made a simultaneous fit of the  $M(D_1^0\pi^+\pi^-)$  and  $M(D_1^+\pi^+\pi^-)$  distributions, where we assume isospin invariance and require the ratio  $N(D_2^*)/N(D_1)$  to be the same for both charge combinations. The fit finds the ratio  $N(D_2^*)/N(D_1) = 0.33 \pm 0.14$  and signal yields of  $N(D_1^0) = 120 \pm 17$ ,  $N(D_1^+) = 107 \pm 16$ . Thus, we set a 90% CL upper limit for  $D_2^*$ :  $\mathcal{B}(B \rightarrow D_2^*\pi^-) \times \mathcal{B}(D_2^* \rightarrow D\pi^+\pi^-) < 0.55\mathcal{B}(B \rightarrow D_1\pi^-) \times \mathcal{B}(D_1 \rightarrow D\pi^+\pi^-)$  [13]. The number of events

for the  $D_1$  mechanism obtained in the fit with the  $\frac{D_2^*}{D_1}$  ratio fixed to 0.46 gives the model uncertainty for the  $D_1$  yield:  ${}_{-21}^{+0}\%$ . Another asymmetric uncertainty, coming from the other possible  $D_1$  sources, is  ${}_{-10}^{+0}\%$  for  $D_1^0$  and  ${}_{-22}^{+0}\%$  for  $D_1^\pm$ . These two uncertainties are combined in the final results as "model" uncertainty.

The signal yields extracted from the  $\Delta E$  distributions are used only for a consistency check of the results. The  $\Delta E$  signal shape is parameterized by a Gaussian with parameters determined from signal MC. The  $\Delta E$  background shape is described by a linear function. We restrict the fit to the range  $-0.1 \text{ GeV} < \Delta E < 0.2 \text{ GeV}$  to avoid contributions from other  $B$  decays, where an additional pion is not reconstructed. Signal yields obtained from the fits to  $\Delta E$  distributions are  $106 \pm 12$  for  $D^0\pi^+\pi^-$  and  $96 \pm 13$  for  $D^+\pi^+\pi^-$ , while the corresponding reconstruction efficiencies are 10.8% and 7.6%, respectively. Thus the obtained reconstructed event numbers by the two methods are consistent within the statistical uncertainty.

In order to determine the total  $D_1 \rightarrow D\pi\pi$  width, analysis of final states with neutral pions is required. With only the  $D_1 \rightarrow D\pi^+\pi^-$  branching fraction measurement, the analysis of the decay dynamics could also be useful to determine the total  $D_1 \rightarrow D\pi\pi$  width. As the limited statistics do not allow us to perform the full amplitude analysis, we consider the one-dimensional projections of several variables:  $M_{D\pi}$ ,  $M_{\pi^+\pi^-}$ ,  $\cos\Theta(\pi_B^-\pi_{D^{**}}^-)$ ,  $\cos\Theta(\pi_B^-\pi_{D^{**}}^+)$ , and  $\cos\Theta(\pi_B^-D)$  (where all angles are calculated in the  $D^{**}$  rest frame). Although these variables are not independent, they highlight each model's features. For instance, the helicity angle distributions differentiate between the  $D_1 \rightarrow D(\pi\pi)$  and  $D_1 \rightarrow (D\pi)\pi$  models. We select events from the  $B$  signal region with the additional requirement  $|M(D\pi\pi) - M_{D_1}| < 25 \text{ MeV}/c^2$ . Decays through the following quasi-two-body intermediate states are considered:  $D_1 \rightarrow D\rho^0 \rightarrow D\pi^+\pi^-$ ,  $D_1 \rightarrow D_0^*(2308)\pi \rightarrow D\pi\pi$  and  $D_1 \rightarrow Df_0(600) \rightarrow D\pi^+\pi^-$  (we set  $M_{f_0} = 0.8 \text{ GeV}/c^2$  and  $\Gamma_{f_0} = 0.8 \text{ GeV}/c^2$ ; the  $D_0^*(2308)$  parameters are taken from Ref. [7]). We use the simplest non-trivial Lorentz-invariant expressions for the corresponding matrix elements in MC simulation [14]. We fit the experimental data with different models. For each variable we plot two distributions: one from the signal region and the other from the  $\Delta E$  sideband. We perform a simultaneous fit to these distributions, assuming a Poisson-like profile in each bin whose mean is the sum of the background and signal (for a given model) in the signal region or the background only in the sideband. The obtained differences of likelihood values for all variables are listed in Table II. Figure 2 shows the  $M_{\pi^+\pi^-}$  and  $\cos\Theta(\pi_B^-D)$  distributions along with expectations based on different  $D_1 \rightarrow D\pi^+\pi^-$  decay models [15]. Although the  $D_1 \rightarrow D_0^*\pi$  decay mechanism describes the data best, some contribution from

TABLE II: Comparison of goodness-of-fit tests for the considered  $D_1 \rightarrow D\pi\pi$  decay models.

Distribution	$(-2 \ln L_{D\rho}/L_{D_0^*\pi})^{1/2}$	$(-2 \ln L_{Df_0}/L_{D_0^*\pi})^{1/2}$
	$D^0, D^+$	$D^0, D^+$
$M_{D\pi}$	2.5, 2.7	1.9, 2.9
$M_{\pi^+\pi^-}$	3.4, 1.6	5.2, 4.7
$\cos\Theta(\pi_B^-\pi_{D^{**}}^+)$	1.6, 2.5	-2.0 <sup>a</sup> , 3.4
$\cos\Theta(\pi_B^-\pi_{D^{**}}^-)$	2.5, 3.0	4.0, 2.9
$\cos\Theta(\pi_B^-D)$	2.0, 0.5	3.2, 4.0

<sup>a</sup>In this case  $L_{Df_0} < L_{D_0^*\pi}$

other mechanisms cannot be excluded completely.

It is interesting to examine the dependence of the  $R$  value on the decay mechanism. The expression for  $R$  can be written as  $s_1 \times \mathcal{B}(B^- \rightarrow D_2^{*0}\pi^-, D_2^{*0} \rightarrow D^{*+}\pi^-) / (s_1 \times \mathcal{B}(B^- \rightarrow D_1^0\pi^-, D_1^0 \rightarrow D^{*+}\pi^-) + s_2 \times \mathcal{B}(B^- \rightarrow D_1^0\pi^-, D_1^0 \rightarrow D^0\pi^+\pi^-))$  where  $s_i$  is a scale factor that recovers the full width from the single decay channel. (It includes branching fractions of other possible decays of both  $D^{**}$  and a meson from its decay products.) Following the procedure used in Ref. [7] and fixing  $s_1$  at 3/2, we can calculate  $s_2$  factors for different models:  $s_2(D^{**0} \rightarrow D_0^{*+}\pi^-) = 9/4$  (disregarding possible interference effects in  $D_1^0 \rightarrow D^+\pi^-\pi^0$  decays),  $s_2(D^{**0} \rightarrow D^0\rho) = 3$ ,  $s_2(D^{**0} \rightarrow D^0f_0) = 3/2$ . Using the branching fractions measured in Ref. [7] and here, the central value for  $R$  depends on the decay model: 0.50 for  $D\rho$ , 0.60 for  $Df_0$  and 0.54 for  $D_0^*\pi$ .

The following sources of systematic errors are considered: tracking efficiency (8% overall, integrated over particle momenta), kaon identification efficiency (2% overall),  $\pi^0$  reconstruction efficiency (8%),  $D$  branching fraction uncertainties (2%-7%), MC statistics (2%), model uncertainty in MC efficiency (10%), uncertainty caused by variation of cuts (5%), background shape uncertainty (10%). The uncertainty in the tracking efficiency is estimated using partially reconstructed  $D^{*+} \rightarrow D^0[K_S^0\pi^+\pi^-]\pi^+$  decays. The kaon identification uncertainty is determined from  $D^{*+} \rightarrow D^0[K^-\pi^+]\pi^+$  decays. The  $\pi^0$  reconstruction uncertainty is obtained using  $D^0$  decays to  $K^-\pi^+$  and  $K^-\pi^+\pi^0$ . To determine the systematic uncertainty in the signal yield extraction, we use different parameterizations for the background events. The overall systematic uncertainty is 19% for  $B \rightarrow D\pi\pi\pi$  and 21% for  $B \rightarrow D^*\pi\pi\pi$ . We assume equal production rates for  $B^+B^-$  and  $B^0\bar{B}^0$  pairs and do not include the corresponding uncertainty in the total systematic error.

The  $B^- \rightarrow D^0\pi^+\pi^-\pi^-$  final state also includes the  $D^{*+}\pi^-\pi^-$  intermediate state with  $D^{*+} \rightarrow D^0\pi^+$ . We reverse the  $D^*$  veto requirement to select  $D^{*+}\pi^+\pi^-$  events and measure the branching ratio  $\mathcal{B}(B^- \rightarrow D^{*+}\pi^-\pi^-) = (1.27 \pm 0.07) \times 10^{-4}$  (based on a sample of  $85 \times 10^6 B\bar{B}$

events), that agrees well with the value of  $\mathcal{B}(B^- \rightarrow D^{*+}\pi^-\pi^-) = (1.25 \pm 0.07) \times 10^{-4}$  measured earlier [7].

In summary, we report the first observation of  $D_1(2420) \rightarrow D\pi^+\pi^-$  decays (with the dominant  $D_1 \rightarrow D^*\pi$  contribution excluded). The measured branching ratios with the corresponding statistical significances and systematic uncertainties are presented in Table I. We find the upper limit for the possible  $D_2^*$  contribution to these results:  $\mathcal{B}(B^- \rightarrow D_2^*\pi^-) \times \mathcal{B}(D_2^* \rightarrow D\pi^+\pi^-) < 0.55\mathcal{B}(B^- \rightarrow D_1\pi^-) \times \mathcal{B}(D_1 \rightarrow D\pi^+\pi^-)$ . No statistically significant signal has been observed for the  $D^{**} \rightarrow D^*\pi^+\pi^-$  decays. The corresponding 90% CL upper limits are listed in Table I. Analysis of the  $D_1 \rightarrow D\pi^+\pi^-$  dynamics shows that the decay model  $D_1 \rightarrow D_0^*\pi$  gives the best description of the data. The  $R = \mathcal{B}(B^- \rightarrow D_2^*\pi^-)/\mathcal{B}(B^- \rightarrow D_1^0\pi^-)$  value calculated assuming  $D_1 \rightarrow D_0^*\pi$  dominates is  $0.54 \pm 0.18$ ; this is  $\sim 2\sigma$  lower than the previously published one.

We thank the KEKB group for the excellent operation of the accelerator, the KEK Cryogenics group for the efficient operation of the solenoid, and the KEK computer group and the NII for valuable computing and SuperSINET network support. We acknowledge support from MEXT and JSPS (Japan); ARC and DEST (Australia); NSFC (contract No. 10175071, China); DST (India); the BK21 program of MOEHRD and the CHEP SRC program of KOSEF (Korea); KBN (contract No. 2P03B 01324, Poland); MIST (Russia); MESS (Slovenia); NSC and MOE (Taiwan); and DOE (USA).

\* on leave from Nova Gorica Polytechnic, Nova Gorica

- [1] S. Eidelman *et al.*, Phys. Lett. B **592**, 1 (2004).
- [2] A.K. Leibovich, Z. Ligeti, I.W. Stewart, M.B. Wise, Phys. Rev. D **57**, 308 (1997).
- [3] M. Neubert, Phys. Lett. B **418**, 173 (1998).
- [4] M.S. Alam *et al.* (CLEO Collaboration), Phys. Rev. D **50**, 43 (1994).
- [5] P. Avery *et al.* (CLEO Collaboration), Phys. Lett. B **331**, 236 (1994) [Erratum-ibid. B **342**, 453 (1995)].
- [6] H. Albrecht *et al.* (ARGUS Collaboration), Phys. Lett. B **232**, 398 (1989).
- [7] K. Abe *et al.* (Belle Collaboration), Phys. Rev. D **69** 112002 (2004).
- [8] S. Kurokawa and E. Kikutani, Nucl. Instr. and Meth. A **499**, 1 (2003).
- [9] A. Abashian *et al.* (Belle Collaboration), Nucl. Instr. and Meth. A **479**, 117 (2002).
- [10] R. Brun *et al.*, GEANT 3.21, CERN DD/EE/84-1, 1984.
- [11] D.M. Asner *et al.* (CLEO Collaboration), Phys. Rev. D **53**, 1039 (1996).
- [12] G.J. Feldman and R.D. Cousins. Phys. Rev. D **57**, 3873 (1998).
- [13] As most of the systematic uncertainties cancel in the ratio of the branching fractions, the systematic uncertainty is

negligible.

- [14] We use the following expressions for matrix elements for

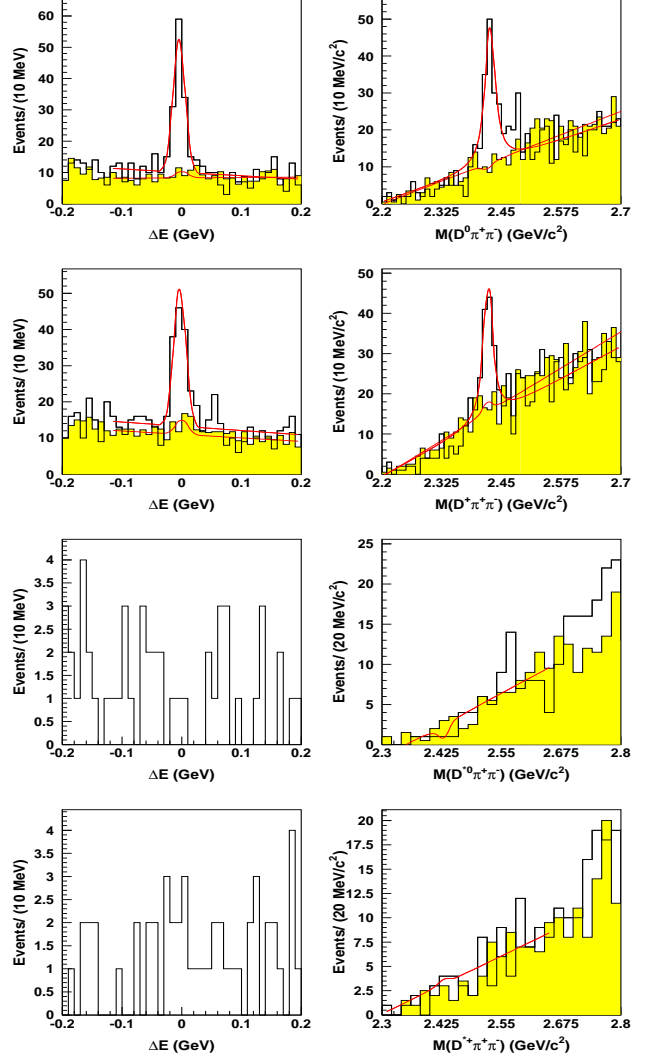


FIG. 1:  $\Delta E$  (left) and  $M_{D\pi\pi}$  (right) distributions for the  $D_1^0 \rightarrow D^0\pi^-\pi^+$  (first row),  $D_1^+ \rightarrow D^+\pi^-\pi^+$  (second row),  $D_1^0 \rightarrow D^{*0}\pi^-\pi^+$  (third row)  $D_1^+ \rightarrow D^{*+}\pi^-\pi^+$  (fourth row). Open histograms represent the data from the signal area, hatched histograms show the  $M_{D\pi\pi}$  (where applicable) and  $\Delta E$  sidebands, respectively, the curves are the fit results - for the signal area and sidebands.

the  $D_1 \rightarrow D\pi\pi$  decay:  $F^{\nu\eta}(B^0, \pi_B^+)F_{\mu\nu}(\bar{D}_0^*, \pi_{D_1^-}^-) \cdot P(D_1^-)_{\eta}P(D_1^-)^{\mu}$ ,  $F^{\phi\eta}(B^0, \pi_B^+)F_{\mu\phi}(f^0, D_1^-) \cdot P(D_1^-)_{\eta}P(D_1^-)^{\mu}$ ,  $F^{\nu\eta}(B^0, \pi_B^+)F_{\nu\mu}(\rho^0, \pi_{\rho^+}^+ - \pi_{\rho^-}^-) \cdot P(D_1^-)_{\eta}P(D_1^-)^{\mu}$ , where the following notation is used:  $F^{\mu\nu}(A, B) = P_A^{\mu}P_B^{\nu} - P_A^{\nu}P_B^{\mu}$ ,  $P(B - C) = P(B) - P(C)$  and  $P$  stands for a 4-momentum.

- [15] In case of the  $Df_0$  model the key  $\cos \Theta(\pi_B^- D)$  distribution is practically independent of the  $f_0$  mass and width.

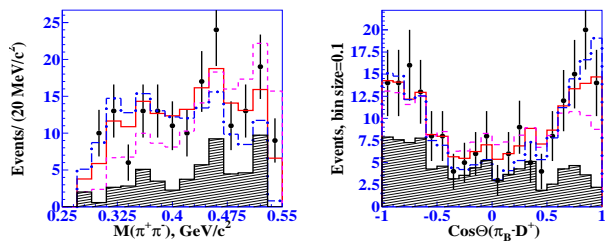


FIG. 2:  $M_{\pi^+\pi^-}$  (left) and  $\cos\Theta(\pi_B^- D^+)$  (right) distributions for the  $D_1^0 \rightarrow D^0 \pi^- \pi^+$  and  $D_1^+ \rightarrow D^+ \pi^- \pi^+$ , respectively. Points with error bars represent the experimental data, solid line -  $D^{*0}\pi$ , dashed -  $D\rho$ , chain -  $Df_0$  models with the expected background added. The hatched histogram corresponds to expected background (from  $\Delta E$  sidebands).